

SPECTRAL, STRUCTURAL AND BIOLOGICAL ANALYSIS OF Cr(III) COMPLEX WITH BENZYLOXYBENZALDEHYDE-4-PHENYL-3-THIOSEMICARBAZONE

B. PRATHIMA,¹ Y. SUBBA RAO,² P.V. CHALAPATHI,³ Y. P. REDDY,⁴ A. VARADA REDDY,^{1*}¹Analytical Division, Department of Chemistry, ² DST-PURSE Centre, S.V. University, ³Department of Chemistry S.V. Arts College, ⁴Department of Physics, SPMVV(Women's University), Tirupati-517502, India. Email: ammireddyv@yahoo.co.in

Received: 15 Jan 2011, Revised and Accepted: 14 Feb 2012

ABSTRACT

The electron paramagnetic resonance (EPR) and optical absorption spectral studies of Cr(III) complex with benzyloxybenzaldehyde-4-phenyl-3-thiosemicarbazone(L) were carried out at room temperature. The ligand was characterized by elemental analysis, IR and ¹H NMR and mass spectra. The EPR data indicated the site symmetry of Cr(III) complex in the crystal to be distorted octahedron. From optical study, the energy values of different orbital levels were estimated. Further the bonding parameters were obtained by correlating optical and EPR data and nature of bonding in the Cr(III) complex were discussed. The values of Racah parameters (B and C) and crystal field parameters (Dq) were obtained to be B = 875 cm⁻¹, C = 3025 cm⁻¹ and Dq = 1531 cm⁻¹. The X-ray powder diffraction indicated triclinic structure with the unit cell parameters a = 8.3109 Å, b = 4.2692 Å, c = 3.5313 Å, V = 120.1 Å³ for the Cr(III) complex. The free ligand and Cr(III) complex was tested for antibacterial activity against gram positive bacteria: *Staphylococcus aureus* and *Bacillus subtilis* and gram negative bacteria: *Klebsiella pneumoniae* and *Escherichia coli*. However with regard to *in vitro* antioxidant activity, the free ligand exhibited greater antioxidant activity than Cr(III) complex.

Keywords: EPR spectra, Electronic spectra, X-ray powder diffraction (XRD), Biological activities.

INTRODUCTION

Thiosemicarbazones, as well as their metal complexes formed the subject of great interest to many researchers for a number of years. Apart from their diverse chemical and structural characteristics, the interest on these compounds also stems from their wide spectrum of biological activity¹, which was already well established. Thiosemicarbazones derivatives and their metallic complexes had extensive biological properties such as antitumor², antifungal antiviral, antibacterial³, antimalaria⁴, anticonvulsant⁵, anti-inflammatory⁶, anti HIV activities⁷. The broad spectra of medicinal properties of this class of compounds were studied for the activity against tuberculosis, leprosy, psoriasis, rheumatism, trypanosomiasis and coccidiosis⁸. Thiosemicarbazones were suggested as pesticides, fungicides and catalysts in chemical and petro-chemical processes⁹. They were used in the analysis of metals for device applications relative to telecommunications, optical computing, optical storage and optical information processing¹⁰. The reason for such pharmacological activities were due to the ability of thiosemicarbazones to chelate strongly with transition metal ions in biological systems binding through thio-keto sulphur and hydrazine nitrogen atoms. Therefore, this type of compounds could coordinate *in vivo* to metal ions. Because of such coordination, the thiosemicarbazone moiety undergoes a sterical reorientation that could favour its biological activities and also thiosemicarbazone complexes diffuse through the semi permeable membrane of the cell lines¹¹.

The present investigation reports synthesis, EPR, Optical, XRD and SEM studies of Cr(III) complex with benzyloxybenzaldehyde-4-phenyl-3-thiosemicarbazone.

MATERIALS AND METHODS

Materials

All the chemicals used were of analytical grade. Organic chemicals such as thiobarbituric acid (TBA), trichloroacetic acid (TCA), α -tocopherol, butylated hydroxy toluene (BHT), 1,1-diphenyl-2-picrylhydrazyl (DPPH), 4-phenyl-3-thiosemicarbazide and dimethylformamide (DMF) were procured from Sigma Aldrich and all metal salts were procured from E. Merck chemical companies.

Physical measurements

The IR spectra of the compounds were recorded on a Nicolet FT-IR 560 Magna spectrometer. The Bruker 300 MHz NMR spectrometer was used to obtain the ¹H NMR spectrum of the ligand. A mass spectrum was recorded in a Quattro LC-Micro mass. Elemental

analysis was obtained from vario-micro qub elemental analyzer. The electronic spectra of the complexes were recorded on a Perkin Elmer UV/VIS Lambda 950. EPR spectra were recorded on an EPR spectrometer (JEOL FE-1X), operating in the X-band frequencies with a modulation frequency of 100 kHz. For EPR measurements, 100 mg of each compound was taken in a quartz tube. The magnetic field was scanned from 2200 to 4200 G, with a scan speed of 250 G min⁻¹. Absorbance was measured using Systronics UV-VIS spectrometer-117. A digital pH meter (model L1-10 Elico, India) was used for measuring pH. X-ray diffractometer (PHILIPSPW3710) using CuK α (1.5418Å) radiation operated at 45kV and 25mA is used in X-ray investigations.

Synthesis of benzyloxybenzaldehyde-4-phenyl-3-thiosemicarbazone

Equal volumes of hot ethanolic solution containing 2.12 g of benzyloxybenzaldehyde and hot ethanolic solution containing 1.67 g of 4-phenyl-3-thiosemicarbazide were mixed. The mixture obtained was refluxed for an hour, then stirred for 3¹/₂ h at 60-70°C and kept at room temperature for a day. The resulting intense yellow colored precipitate was filtered, washed with ethanol and dried. The schematic structure is depicted below.

Synthesis of Cr(III) complex

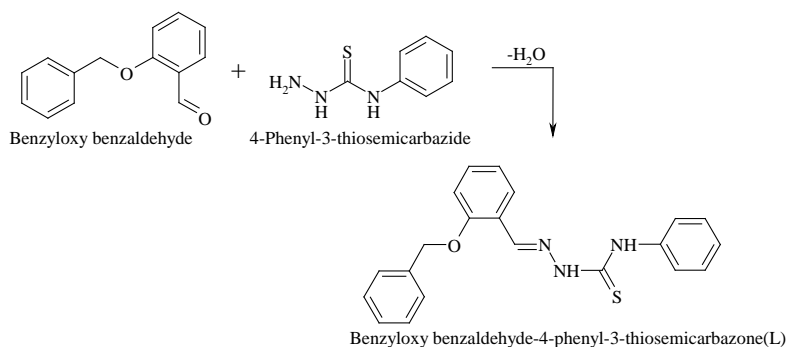
A mixture of hot ethanolic solution (10 ml) of free ligand (0.01 mol) and a hot ethanolic solution (10 ml) of the CrCl₃.6H₂O (0.02 mol) was refluxed for 2¹/₂ h at 60°C. The resulting solution was allowed to stand at room temperature and upon slow evaporation gives Dark green colored crystals. The crystals formed were washed with 50% ethanol and dried. The purity of the complex was checked by TLC.

Antibacterial screening

In vitro antibacterial screening was performed by the agar disc diffusion method^{12,13}. The bacterial species used in the screening were gram-negative bacteria such as *Klebsiella pneumoniae* and *Escherichia coli* and gram-positive bacteria such as *Staphylococcus aureus* and *Bacillus subtilis*. Stock cultures of the test bacterial species were maintained on nutrient agar media (Hi-media laboratories, Mumbai) by sub culturing in Petri dishes. The media were prepared by adding the components as per manufacturer's instructions and sterilized in the autoclave at 121°C and atmospheric pressure for 15 min. Each medium was cooled to 45-60°C and 20 ml of it was poured into a Petri dish and allowed to solidify. After solidification, Petri plates with media were spread with 1.0 ml of bacterial suspension prepared in sterile distilled

water. The wells were bored with cork borer and the agar plugs were removed. To each agar well, 100 ml of the compound reconstituted in DMF of concentration 1.0 mg/ml was added. DMF was used as a negative control and in similar way, antibiotics such as ampicillin and tetracycline were used as positive control standards. All the plates were incubated at 37°C for 24 h and they

are observed for the growth inhibition zones. The presence of clear zones around the wells indicated that both the ligand and complex were active. The diameter of zone of inhibition is calculated in millimeters. The well diameter was deducted from the zone diameter to get the actual zone of inhibition diameter and the values were tabulated.



DPPH scavenging activity

The principle for the reduction in DPPH free radicals was that the antioxidant reacts with stable free radical DPPH and converts it to 1,1-diphenyl-2-picrylhydrazine. The ability to scavenge the stable free radical DPPH is measured by decrease in the absorbance at 517 nm. Solutions of ligand and Cr(III) complex at 100 μ M concentrations were added to 100 μ M DPPH and kept in ethanol tubes. The tubes were kept at ambient temperature for 20 min and absorbances were measured at 517 nm. For positive control, α -tocopherol was used¹⁴. These measurements were run in triplicate. The percentage of scavenging activity was calculated as follows:

$$\text{Scavenging activity (\%)} = [(A_{\text{DPPH}} - A_{\text{TEST}}) / A_{\text{DPPH}}] \times 100$$

where A_{DPPH} is the absorbance of DPPH without test sample (control) and A_{TEST} is the absorbance of DPPH in the presence of test sample.

Inhibition of lipid peroxidation in rat brain homogenate

Preparation of rat brain homogenate

For the present study, Albino Wistar rats (180-200g) were selected. Prior to decapitation and removal of the brain, the animals were anesthetized with ether and perfused transcardially with ice-cold normal saline to prevent contamination of brain tissue with blood. The collected tissues were weighed and their homogenates (10% w/v) were prepared in 0.15 M KCl and centrifuged at 800 rpm for 10 min. The supernatants were used immediately for the study¹⁵.

Iron(III) induced lipid peroxidation

The incubation mixtures contain a final volume of 1.5 ml brain homogenate (0.5 ml of 10% w/v), KCl (0.15 M) and ethanol (10 μ l) or test compound dissolved in ethanol. Peroxidation was initiated by adding ferric chloride (100 μ M) to give the final concentration

stated. After incubation for 20 min at 37°C, reactions were stopped by adding 2 ml of ice-cold 0.25 M HCl containing 15% trichloroacetic acid (TCA), 0.38% thiobarbituric acid (TBA) and 0.05% butylated hydroxy toluene (BHT). The samples were heated at 80°C for 15 min, cooled and centrifuged at 1000 rpm for 10 min. The absorbances of the supernatant solutions were measured at 532 nm. Percentage inhibition of thiobarbituric acid reactive substances (TBARS) formed by test compounds were calculated by comparing with the control. Iron(III) solutions were prepared afresh in distilled water and other solutions are prepared in 0.15 M KCl. Since most buffers trap hydroxyl radical or interfere with iron conversion, the reactions were carried out in unbuffered 0.15 M KCl solution^{16,17}.

The inhibition percentages of the selected ligand and Cr(III) complex were evaluated using lipid peroxidation method. The following formula was used in calculating inhibition percentages.

$$\text{Inhibition percentage} = [(A_{\text{CONT}} - A_{\text{TEST}}) / A_{\text{CONT}}] \times 100$$

Here, A_{CONT} is the absorbance of the control reaction and A_{TEST} is the absorbance in the presence of the test sample.

RESULTS AND DISCUSSION

Spectral characterization of ligand and its Cr(III) complex

Benzoyloxybenzaldehyde-4-phenyl-3-thiosemicarbazone(L) was analyzed by ¹H-NMR spectrum of ligand (Fig. 1) investigations provide the following information 8.0-7.15 (m, 14H, Ar-H), 11.66 (s, NH), 5.13 (s, N = CH), 3.12 (s, OCH₂). The mass spectrum of ligand (Fig. 2) exhibited a molecular ion (M⁺) peak at m/z value is 362.1, corresponding to the species [C₂₁H₁₉N₃OS]⁺, which confirmed the proposed formula. The ligand and Cr(III) complex were isolated as coloured air stable derivatives with acceptable melting points and the Physical data given in Table 1.

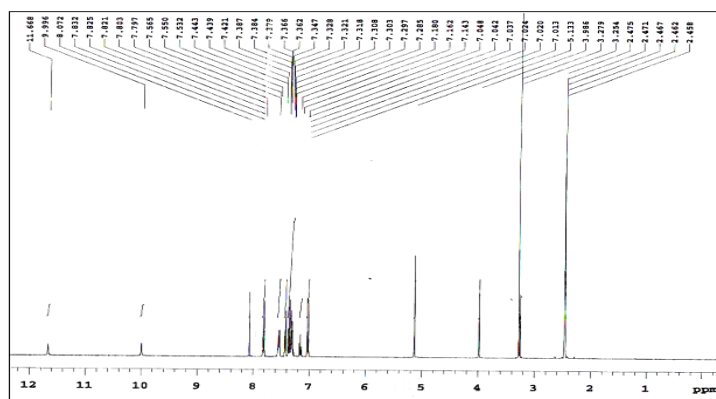


Fig. 1: ¹H-NMR spectrum of the free ligand

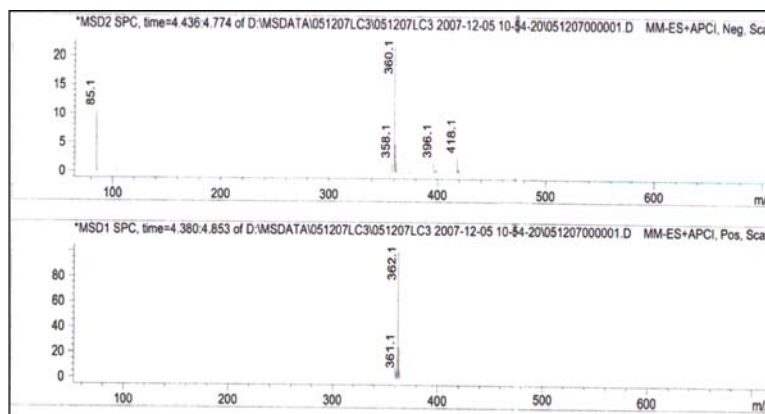


Fig. 2: Mass spectrum of the free ligand.

Table 1: Reaction condition and their Physical data of ligand and its Cr(III) complex

Compound formed	Reaction time(hrs)	Reaction Temp(°C)	Color	Yield (%)
Ligand(L)	3 ¹ / ₂	60-70	Yellow	87
[Cr(L) ₂ Cl ₂]Cl	2 ¹ / ₂	50	Dark green	62

The molar conductance value of the Cr(III) complex was 47 mho mole⁻¹ cm², it indicated electrolytic behavior. The analytical data for metal, carbon, hydrogen and nitrogen in the ligand and

Cr(III) complex were presented in Table 2. The theoretical values of elements in the corresponding Cr(III) complex were calculated on the assumption that the metal combines with the ligand in 1:2 ratio.

Table 2: Analytical data of ligand and its Cr(III) complex

Compound	Analytical data % found (calculated)				
	M	C	H	N	S
ligand	-	69.78 (69.32)	5.30 (5.043)	11.63 (11.35)	8.87 (8.725)
[Cr(L) ₂ Cl ₂]Cl	5.91 (5.88)	57.35 (57.23)	4.42 (4.34)	9.58 (9.53)	7.31 (7.27)

The binding mode of ligand to its metal complex was studied by comparing the infrared spectrum of free ligand (L) with the spectrum of complex. Important spectral bands were presented in Table 3. Typical IR spectra of ligand and Cr(III) complex were given in Figs. 3 and 4 respectively. The IR spectrum of free ligand exhibited band in 3307 cm⁻¹ region which could be attributed to the ν(-NH) vibration. In the spectrum of the ligand, a strong band was observed in 1253 cm⁻¹ region corresponding to ν(C=S) and no bands were observed near 2700-2500 cm⁻¹ suggesting that the free ligand

remains in thione form in the solid state. In IR spectra of complexes, ν(C=S) band has disappeared and new bands are observed in the region of 1228 cm⁻¹. This indicated the bond formation between metal and sulphur atom in the Cr(III) complex. A strong band was observed in 1590-1610 cm⁻¹ region, in the IR spectrum of free ligand. This band shift to lower frequency in IR spectra of complexes suggested the involvement of azomethine nitrogen ν(C=N-) in chelation¹⁸. The non-ligand bands in 600-400 cm⁻¹ region were assigned to ν(M-N) and ν(M-S) modes^{19,20}.

Table 3: Important IR (cm⁻¹) bands of free ligand and Cr(III) complex

Compound	ν(-NH)	ν(C=N-)	ν(C=S)	ν(M-N)	ν(M-S)
Ligand(L)	3307	1598-1543	1253	-	-
[Cr(L) ₂ Cl ₂]Cl	3329	1580	1234	459	416

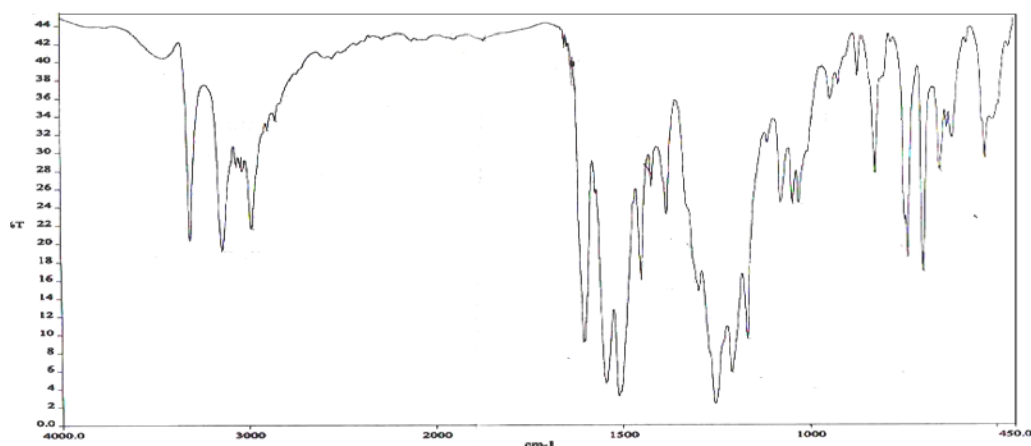


Fig. 3: IR spectrum of Ligand.

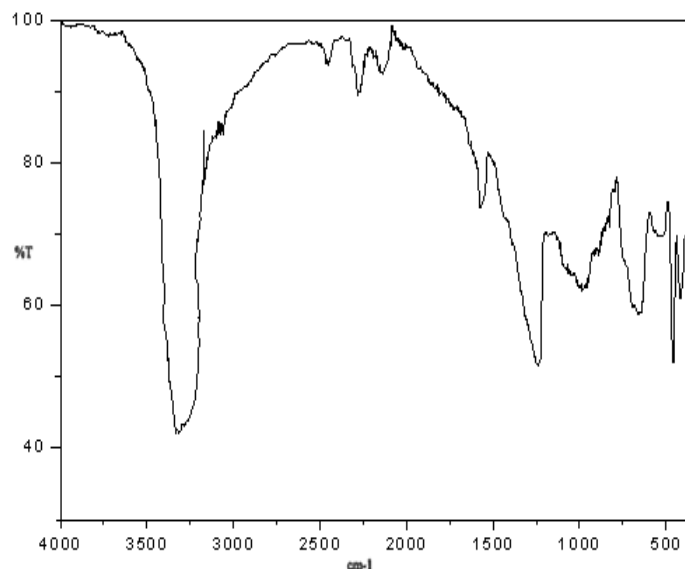


Fig. 4: IR spectrum of Cr(III) complex.

EPR and Optical studies

The EPR spectrum of the chromium(III) complex was recorded at room temperature with polycrystalline sample, in X-band at 9.205GHz in the magnetic field range 2200-4200G. The EPR spectrum (Fig. 5) for chromium(III) complex in solid form exhibited a broad signal at g value 1.998, confirming the presence of hexa coordinated chromium(III) centers.

Optical absorption spectra of Cr(III) at the room temperature (RT) were shown in (Fig. 6). The broad bands observed at 653 and 433 nm were attributed to the spin allowed transitions ${}^4A_{2g}(F) \rightarrow {}^4T_{2g}(F)$ and ${}^4A_{2g}(F) \rightarrow {}^4T_{1g}(F)$ respectively, corresponding to the transition ${}^4A_{2g}(F) \rightarrow {}^4T_{2g}(F)$ gives the 10 Dq value. The wave number (23088 cm^{-1} ; ν_2) of the band correspond to ${}^4A_{2g}(F) \rightarrow {}^4T_{1g}(F)$ transition. Using the following formula $B = (2 \nu_1 \nu_2 + \nu_2 - 3$

$\nu_1 \nu_2) / (15 \nu_2 - 27 \nu_1)$, the value of B was evaluated and found to be 875 cm^{-1} . The other weak bands of the spin forbidden transitions from ${}^4A_{2g}(F)$ to ${}^2E_g(G)$, ${}^2T_{2g}(G)$ and ${}^4T_{1g}(P)$ were attributed at 687, 448 and 273 nm respectively. The ${}^4A_{2g}$, 2E_g and ${}^2T_{1g}$ terms result from the same configuration t_{2g}^3 . The bands corresponding to an electron jump between these states arising from the same configuration were expected to be sharp. Therefore the assignments of the sharp band observed at 687 nm to the transition ${}^4A_{2g}(F) \rightarrow {}^2E_g(G)$ were in tune with the theoretical prediction. Based on the above assignments the Tanabe-Sugano matrices²¹ for different values of Dq, B and C were solved and the following values were in good agreement between the calculated and observed band positions: $Dq = 1531$ B = 875 and $C = 3025 \text{ cm}^{-1}$. The band head data along with their assignments was presented in Table 4.

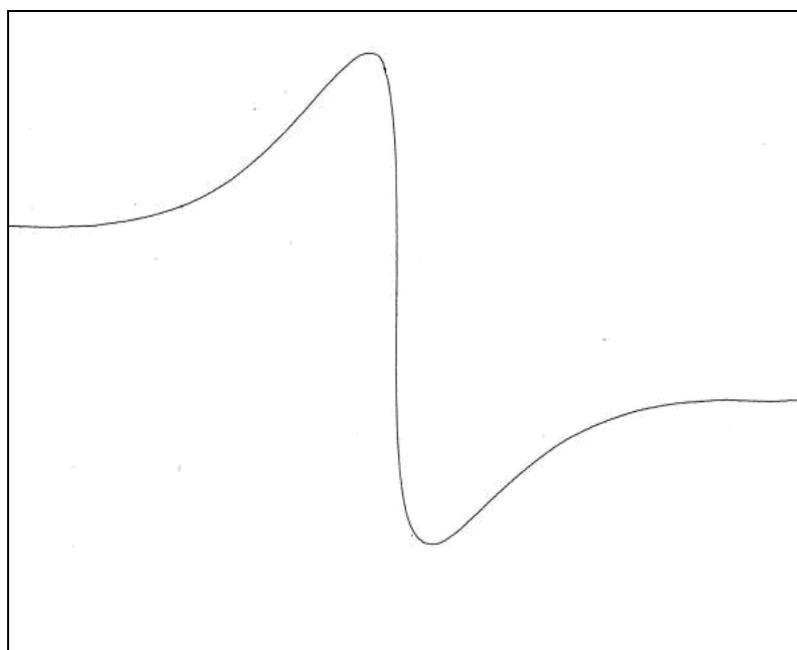


Fig. 5: Powder X-band EPR spectrum of Cr(III) at room temperature ($\nu = 9.205\text{GHz}$).

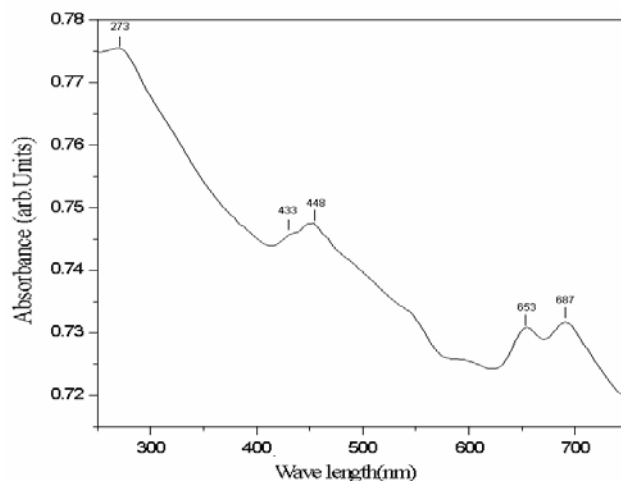


Fig. 6: Solid state electronic absorption spectrum (nm) of Cr(III) complex.

Table 4: Observed and calculated band positions of Cr(III) complex

Transition From ${}^4A_{2g}(F) \rightarrow$	Observed Bands Wavelength (nm) Wave number (cm^{-1})	Calculated bands Wave number (cm^{-1})
${}^4T_{1g}(P)$	273 36620	35960
${}^4T_{1g}(F)$	433 23088	23095
${}^2T_{2g}(G)$	448 22315	22419
${}^4T_{2g}(F)$	653 15310	15310
${}^2E_g(G)$	687 14552	15240

Powder X-ray Diffraction

X-ray diffraction was performed to obtain further evidence about the structure of the Cr(III) complex. The diffractogram obtained for the free ligand and Cr(III) complex were given in Figs. 7 and the XRD patterns indicated crystalline nature for the free ligand and Cr(III) complex. The observed and calculated 'd' values, 2θ angles and (h k l) values were listed in Table 5. The observed X-ray pattern of the free ligand sample studied in the present investigation indicated amorphous nature. The Cr(III) complex crystallized in triclinic type of lattice with dimensions as $a = 8.3109 \text{ \AA}$, $b = 4.2692 \text{ \AA}$, $c = 3.5313 \text{ \AA}$, $\alpha = 99.085^\circ$, $\beta = 94.564^\circ$, $\gamma = 102.145^\circ$ and cell volume $V = 120.1 \text{ \AA}^3$. To evaluate the crystallite size of the synthesized Cr(III) complex, D was determined using Debye-Scherrer formula²² given by

$$D = \frac{0.94\lambda}{\beta \cos \theta} \quad (1)$$

where β is the full width at half maximum of the predominant peak and θ is the diffraction angle and λ is the wavelength of light. The full width at half maximum intensity corresponding to the plane (211) of the pattern was considered for calculation. The sizes of the crystallites of the Cr(III) complex were found to be of the order of 50 nm.

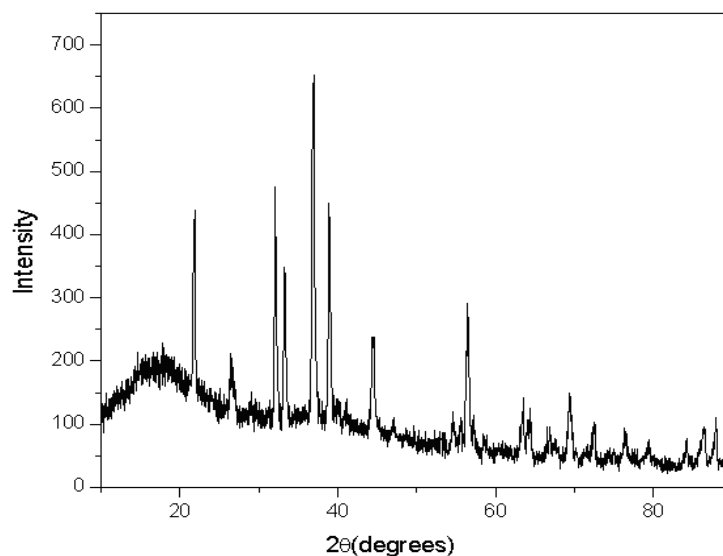


Fig. 7: XRD spectrum of Cr(III) complex.

Table 5: Powder X-ray diffraction data of Cr(III) complex

Peak number	d-spacing (Å)		2θ values		Δ 2θ	(hkl) (99)
	Observed	Calculated	Observed	Calculated		
1	4.1061	4.1061	21.62	21.62	0.000	(010)
2	4.0490	4.0490	21.93	21.93	0.000	($\bar{1}$ 10)
3	3.3645	3.3645	26.47	26.47	0.000	(110)
4	3.3264	3.3264	26.78	26.78	0.000	($\bar{1}$ 01)
5	3.0556	3.0556	29.20	29.20	0.000	(101)
6	2.8002	2.8002	31.93	31.93	0.000	($\bar{1}$ 11)
7	2.4432	2.4405	36.75	36.80	-0.043	(011)
8	2.2976	2.2969	39.17	39.19	-0.011	($\bar{2}$ 11)
9	2.0416	2.0412	44.33	44.34	-0.011	($\bar{3}$ 11)
10	1.6790	1.6790	54.61	54.61	-0.001	($\bar{1}$ 12)
11	1.6371	1.6360	56.13	56.17	-0.039	($\bar{4}$ 20)
12	1.4663	1.4659	63.38	63.40	-0.022	($\bar{3}$ 21)
13	1.3034	1.3035	72.45	72.45	0.001	($\bar{6}$ 11)
14	1.2457	1.2453	76.39	76.42	-0.029	($\bar{2}$ 22)
15	1.1483	1.1485	84.25	84.24	0.014	($\bar{4}$ 22)
16	1.0923	2.7138	89.69	89.68	0.006	($\bar{3}$ 13)

Scanning electron microscopy (SEM)

Scanning electron micrography was used to evaluate morphology the free ligand and Cr(III) complex. SEM images of the synthesized benzyloxybenzaldehyde-4-phenyl-3-thiosemicarbazone and the corresponding Cr(III) complex were in Figs. 8 and 9 respectively. The SEM micrographs of the free ligand and Cr(III) complex. The SEM image of free ligand consists of irregular spherical particles and all the particles were dispersed very well, where as Cr(III) complex exhibited irregular morphology.

Antibacterial activity

Antibacterial activity of the ligand and its Cr(III) complex were tested against different micro-organisms. The activities of the ligand and its Cr(III) complex were compared with standard antibiotics such as ampicillin and tetracycline as given in Table 6. The Cr(III) complex had shown a good activity against gram-negative bacteria (*Escherichia coli* and *Klebsiella pneumonia*) and gram-positive bacteria (*Staphylococcus aureus* and *Bacillus subtilis*).

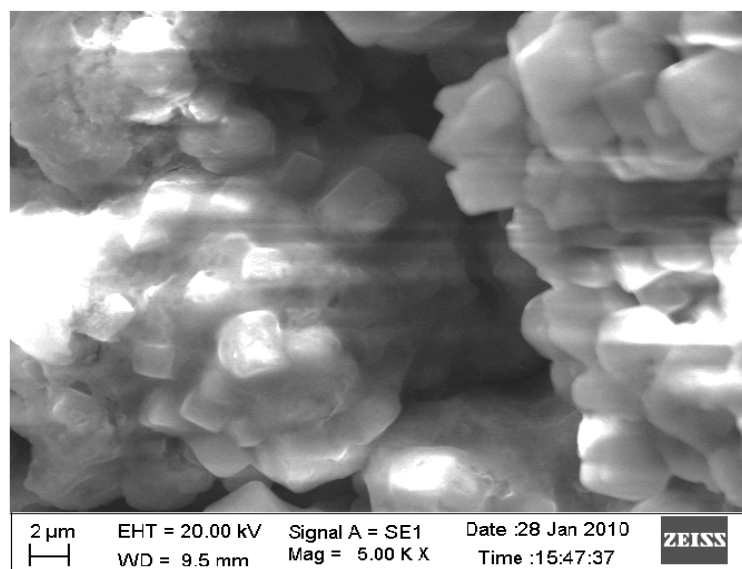


Fig. 8: The SEM image of the free ligand

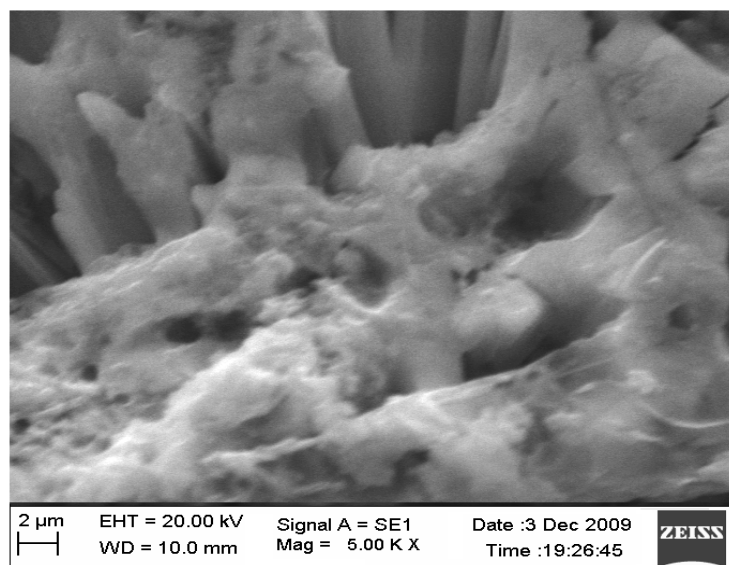


Fig. 9: The SEM image of the Cr(III) complex.

Table 6: Antibacterial screening data of the ligand and Cr(III) complex (Diameter of zone of inhibition in mm)

Compound	K. Pnuemoniae	E. Coli	B. Subtilis	S. Aureus
Ligand(L)	-	-	-	-
[Cr(L) ₂ Cl ₂]Cl	22	16	06	28
Ampicillin	43	40	43	42
Tetracycline	32	33	30	32

The synthesized ligand and its Cr(III) complex were screened for reduction in DPPH free radicals and inhibition of iron(III) induced lipid peroxidation at 100 μm concentration. The free ligand exhibited comparable activity in DPPH scavenging and ferric ion

induced lipid peroxidation as seen in the case of standard antioxidant α-tocopherol, but Cr(III) complex has not shown any activity as given in Table 7.

Table 7: Effect of ligand and its metal complexes on scavenging of DPPH and Fe³⁺ induced lipid peroxidation at 100 μM concentration

Compound	DPPH scavenging (%)	Fe ³⁺ induced lipid peroxidation
Ligand(L)	42	60
[Cr(L) ₂ Cl ₂]Cl	-	-
α-tocopherol	53	65

CONCLUSIONS

The title ligand benzyloxybenzaldehyde-4-phenyl-3-thiosemicarbazone was synthesized and its structure was investigated. The Cr(III) complex was prepared with the ligand and they were characterized with analytical and spectral techniques. The EPR and electronic spectral studies of the Cr(III) complex indicated near octahedral site symmetry for the metal ion. The ligand did not exhibit any antibacterial activity but its Cr(III) complex exhibited considerable antibacterial activity. Free ligand exhibited good activity in DPPH scavenging and ferric ion induced lipid peroxidation, but the Cr(III) complex did not exhibit these activities.

ACKNOWLEDGEMENT

The authors wish to acknowledge financial support received from DST-PURSE (Govt. of India) S.V. University, Tirupati and UGC-BSR New Delhi. They also sincerely thank Prof. J. Lakshmana Rao, Department of Physics, S. V. University, Tirupati, for his help in EPR studies.

REFERENCES

1. Mohammad MH, Foysal AMD, Rehana A, Mahabub H, Abdullahil M, Taksim A, Ehsanul hoque mazumder MD. In vitro free

- radical scavenging activity of some β-lactams and phenolics, Int J Pharmacy Pharm Sci. 2010; 2: 60-63.
- Sreekanth T, Subhas SK, Babu rao B. Synthesis, characterization and antibacterial activity of some novel mononuclear Ru(II) complexes, Int J Pharmacy Pharm Sci. 2009; 1: 62-70.
 - Sriram D, Bal TR, Yogeesswari P. Synthesis, antiviral and antibacterial activities of isatin mannich bases, Med. Chem. Res. 2005; 14:11-28.
 - Lopes F, Capela R, Goncaves JO, Horton PN, Hursthouse MB, Iley J, Casimiro CM, Bom J, Moreire R. Amidomethylation of amodiaquine: antimalarial N-mannich base derivatives, Tetrahedron Letters. 2004; 45: 7663-7666.
 - Chinnasamy Rajaram Prakash, Sundararajan Raja, Govindaraj Saravanan, Synthesis, characterization and anticonvulsant activity of novel schiff base of isatin derivatives, Int J Pharmacy Pharm Sci. 2010; 2:177-181.
 - Bhattacharya SK, Chakrabarti S. Dose-related proconvulsant and anticonvulsant activity of isatin, a putative biological factor in rats, Ind J Exp. Biol. 1998; 36: 118-121.
 - Pandeya SN, Sriram D, DeClercq E, Nath G. Synthesis, antibacterial, antifungal and anti-HIV activities of schiff and mannich bases derived from isatin derivatives and N-[4-(4'-chlorophenyl)thiazol-2-yl]thiosemicarbazide, Eur J Pharm Sci. 1999; 9: 25-31.

8. Demertzi DK, Domopoulou A, Demertzis MA, Valle G, Papageorgiou AJ. Palladium(II) complexes of 2-acetylpyridine N(4)-methyl, N(4)-ethyl and N(4)-phenyl-thiosemicarbazones. Crystal structure of chloro(2-acetylpyridine N(4)-methylthiosemicarbazonato) palladium(II). Synthesis, spectral studies, in vitro and in vivo antitumour activity, J Inorg. Biochem. 1997; 68: 147-155.
9. Latika D, Singh RV. Synthesis, Spectroscopic Characterization, Antimicrobial, Pesticidal and Nematicidal Activity of Some Nitrogen-Oxygen and Nitrogen-Sulfur donor Coumarins based Ligands and their Organotin(IV) Complexes, Appl. Organomet. Chem. 2011; 25: 643-652.
10. El Mostapha Jouad, Amédée Riou, Magali Allain, Mustayeen A Khan, Gilles M Bouet, Synthesis, structural and spectral studies of 5-methyl 2-furaldehyde thiosemicarbazone and its Co, Ni, Cu and Cd complexes. Polyhedron; 2001; 20: 67-74.
11. Ahmed AA, Mohammad MH, Mohammad H, Abdel-Rhman. Synthesis, characterization and antibacterial activity of Pd(II), Pt(II) and Ag(I) complexes of 4-ethyl and 4-(*p*-tolyl)-1-(pyridin-2-yl)thiosemicarbazides. Journal of Sulfur Chemistry; 2010; 31: 141-151
12. Bauer AW, Kirby WM, Sherris JC, Turck M. Antibiotic susceptibility testing by a standardized single disk method, Am J Clin Pathol, 1966; 45: 493-496.
13. Sheikh C, Hossain M S, Easmin, MS, Islam, MS, Rashid M. Evaluation of in vitro antimicrobial and in vivo cytotoxic properties of some novel titanium-based coordination complexes, Biological & Pharmaceutical Bulletin, 2004; 27: 710-713.
14. Baliga MS, Jagetia GC, Venkatesh P, Reddy R, Ulloor JN, Radioprotective effect of abana, a polyherbal drug following total body irradiation, Brit. J Radiol, 2004; 77: 1027-1035.
15. Bharathi K, Swarnalatha G, Begum SKA, Prasad K. Synthesis and antioxidant activity substituted 1-acetyl-5-(substituted phenyl)-3-(amino phenyl)-2-pyrazolines and 5-(substituted phenyl)-3-(amino phenyl) isoxazolines. J Pharm. Res, 2008; 7: 78-81.
16. Braugher JM, Robin L, Chase PJF. Stimulation and inhibition of iron-dependent lipid peroxidation by desferrioxamine. Biochemical and Biophysical Research Communications, 1988; 153: 933-938.
17. Jayan S, Rao MNA. Curcuminoids as potent inhibitors of lipid peroxidation. J Pharmacy Pharmacol, 1994; 46: 1013-1016.
18. West DX, Swearingen JK, Valdes-Martinez J, Hernandez-Ortega S, El-Sawaf A K, Van Meurs F, Castineiras A, Garcia I, Bermejo E, Spectral and structural studies of iron(III), cobalt(II,III) and nickel(II) complexes of 2-pyridineformamide-N(4)-methylthiosemicarbazone. Polyhedron, 1999; 18: 2919-2929.
19. Chandra S, Anil kumar G, Spectral, IR and magnetic studies of Mn(II), Co(II), Ni(II) and Cu(II) complexes with pyrrole-2-carboxyaldehydethiosemicarbazone. Spectrochimica Acta, part A, 2007; 68: 469-473.
20. Chandra S, Kumar U, Verma HS. Cobalt(II) complexes of semicarbazones and thiosemicarbazones. J Saud. Chem. Soc, 2003; 7: 337-346.
21. Tanabe Y, Sugano S. J. Phys. Soc. Jpn, 1954; 9: 753-766.
22. Warren BE, In: X-ray Diffraction. Dover, New York, 1990; 253.